HHS Public Access

Author manuscript

Dev Biol. Author manuscript; available in PMC 2015 September 15.

Published in final edited form as:

Dev Biol. 2014 September 15; 393(2): 298–311. doi:10.1016/j.ydbio.2014.06.025.

GRAF1 promotes ferlin-dependent myoblast fusion

Kaitlin C. Lenhart[a], **Abby L. Becherer**[a], **Jianbin Li**[b], **Xiao Xiao**[b], **Elizabeth M. McNally**[c], **Christopher P. Mack**[a,d], and **Joan M. Taylor**[a,d,*]

[a]Department of Pathology and Laboratory, Medicine, The University of North Carolina at Chapel Hill, Chapel Hill, NC, 27599, USA

[b]Department of Gene Therapy Molecular Pharmaceutics, The University of North Carolina at Chapel Hill, Chapel Hill, NC, 27599, USA

[c]Department of Medicine, The University of Chicago, Chicago, IL, USA

[d]McAllister Heart Institute, University of North Carolina at Chapel Hill, Chapel Hill, NC 27599, USA

Abstract

Myoblast fusion (a critical process by which muscles grow) occurs in a multi-step fashion that requires actin and membrane remodeling; but important questions remain regarding the spatial/temporal regulation of and interrelationship between these processes. We recently reported that the Rho-GAP, GRAF1, was particularly abundant in muscles undergoing fusion to form multinucleated fibers and that enforced expression of GRAF1 in cultured myoblasts induced robust fusion by a process that required GAP-dependent actin remodeling and BAR domain-dependent membrane sculpting. Herein we developed a novel line of GRAF1-deficient mice to explore a role for this protein in the formation/maturation of myotubes *in vivo*. Post-natal muscles from GRAF1-depleted mice exhibited a significant and persistent reduction in cross-sectional area, impaired regenerative capacity and a significant decrease in force production indicative of lack of efficient myoblast fusion. A significant fusion defect was recapitulated in isolated myoblasts depleted of GRAF1 or its closely related family member GRAF2. Mechanistically, we show that GRAF1 and 2 facilitate myoblast fusion, at least in part, by promoting vesicle-mediated translocation of fusogenic ferlin proteins to the plasma membrane.

Keywords

GRAF; Endocytic recycling; Ferlin; Myoblast fusion

Introduction

Myogenesis occurs through the fusion of singly nucleated myoblasts into multinucleated myotubes and this process is essential for proper skeletal muscle formation and injury repair. It is becoming clear that dynamic and coordinated changes in actin polymerization and

*Corrrespondence to: 501 Brinkhous-Bullitt Bld, University of North Carolina, CB7525,Chapel Hill, NC 27599, USA. Fax: +1 919 966 6718. jmt3x@med.unc.edu (J.M. Taylor).

vesicle trafficking are required for skeletal muscle formation. For example, formation and subsequent dissolution of an F-actin focus at the distal ends of fusion competent myoblasts is essential for myoblast-myoblast fusion (Peckham, 2008; Schafer et al., 2007; Schroter et al., 2004; Swailes et al., 2004). The dissolution of actin is thought to be important for promoting intercellular lipid bilayer fusion and perhaps for the recruitment of unilamellar vesicles that deposit essential fusogenic proteins and phospholipids (Kalderon and Gilula, 1979), but the molecular machinery that orchestrate coordinated changes in vesicular trafficking and actin dynamics remain elusive.

Myoferlin and its family members (dysferlin and Fer1L5) are large membrane anchored proteins that contains six to seven calcium response domains (so-called C2 domains) and their structures closely resemble that of synaptotagmins, proteins that facilitate fusion of membrane-bound vesicles to the plasma membrane during exocytic neurotransmitter release (Martens et al., 2007). Dysferlin-deficiency is causal for Limb girdle muscular dystrophy 2B, and studies in muscle fibers lacking dysferlin revealed defects in membrane resealing following mechanical or laser-induced membrane rupture (Bansal et al., 2003; Han and Campbell, 2007). The finding that dysferlin-null muscle retained accumulation of vesicles near membrane damage sites indicates that dysferlin likely mediates the final step of fusion necessary for plasma membrane repair (Posey et al., 2011b). Myoferlin and Fer1L5 which are transiently expressed during myogenesis and are known to facilitate myoblast fusion during the development of nascent muscle fibers likely function in a similar fashion. Ferlins are only transiently expressed on muscle plasma membranes and their active recruitment to the sarcolemma is tightly regulated by endocytic recycling mediated by the Eps15 homology domain (EHD)-containing proteins 1 and 2 (Cai et al., 2009a; Doherty et al., 2008; Posey et al., 2011a, 2011b). While several muscular dystrophies are associated with abnormal plasma membrane localization of dysferlin, indicating the significance of this regulatory process (Cai et al., 2009b; Evesson et al., 2010; Matsuda et al., 2001; Wallace and McNally, 2009), the precise mechanisms that govern ferlin recruitment during myoblast fusion or to sites of injury are still poorly understood.

We recently identified a striated muscle enriched protein termed GRAF1 that is poised to co-regulate actin- and lipid-dynamics by virtue of its multi-domain structure that includes a N-terminal lipid binding/bending BAR domain, a phosphatidyl serine (PS)-binding PH domain, a central Rho-GAP domain, and a C-terminal protein-interaction SH3 domain that interacts with focal adhesion kinase (FAK) (Hildebrand et al., 1996; Taylor et al., 1998, 1999). We reported that depletion of GRAF1 from developing tadpoles induced a highly penetrable dystrophic phenotype that that led to immobility (Doherty et al., 2011). Moreover, we showed that ectopic expression of GRAF1 in cultured myoblasts induced robust fusion by a process that required both GAP-dependent actin remodeling and BAR domain-dependent membrane binding or sculpting. However, since myoblast fusion does not occur in developing tadpoles, questions remained as to whether (or to what extent) GRAF1 was necessary for myoblast fusion *in vivo*. We developed a novel line of GRAF1 deficient mice and our studies detailed herein reveal that while viable, these mice exhibit limited myogenesis. Moreover, our mechanistic studies reveal that GRAF1 and its related

family member, GRAF2, regulate myoblast fusion by promoting endocytic recycling-dependent membrane recruitment of the fusogenic ferlin proteins to the plasma membrane.

Materials and methods

Generation of GRAF1 gene trap mice

GRAF1 gene trap mice were generated and obtained from the Texas A&M Institute for Genomic Medicine (College Station, TX) using the OmniBank ES cell clone OST135790 which harbors the gene trapping vector VICTR48 within the first intron of *Graf1* (*Arhgap26*, accession #: NM_175164). To generate a stable mutant mouse line, 129SvEv-derived ES cells were microinjected into host C57BL/6J mice for germline transmission of the *GRAF1* mutation. All experimental mice were maintained on a mixed 129/SvEv-C57BL/6J genetic background. Mice were genotyped utilizing the following primers: forward Primer A (5-AGCACTGTGAACACCATTCTG-3′), forward Primer C (5′-AAATGGCGTTACTTAAGCTAGCTTGC-3′), and reverse Primer B (5′-AAAGGACATCTGACACTACCAAA-3′). Animals were treated in accordance with the approved protocol of the University of North Carolina (Chapel Hill, NC) Institutional Animal Care and Use Committee, which is in compliance with the standards outlined in the guide for the Care and Use of Laboratory Animals.

Primary antibodies and cDNA constructs

Commercial antibodies were purchased from Sigma (laminin, tropomyosin (CH1) and monoclonal γ-tubulin); Abcam (EHD2, Lamp2 and Thy-1); BD Biosciences (GM130 and Rab5); Epitomics (EHD1); Cell Signaling (Myc-tag, 9B11); GAPDH (Imgenex); Novus Biologicals (myoferlin); and Developmental Studies Hybridoma Back, Univ. of Iowa (MHC, NA4). The GRAF2 (PS-GAP) antibody was a generous gift from Dr. Wen-Cheng Xiong (Georgia Regents University, GA) (Ren et al., 2001). Derivation of the polyclonal Fer1L5 and GRAF1 antibodies was previously described (Doherty et al., 2011; Posey et al., 2011b). A hamster monoclonal GRAF1 antibody was designed in house using the identical peptide immunogen by standard methodology. The GRAF1^{loxP} cDNA construct was described (DiMichele et al., 2009; Doherty et al., 2011). Briefly, Myc-tagged GRAF1 was subcloned into a Cre recombinase-inducible construct, downstream of a beta-actin promoter and a GFP reporter followed by a transcriptional ‘stop’ site flanked as a unit by loxP sites. As such, the GRAF1^{loxP} construct allows for Cre-dependent expression of GRAF1 in a time-dependent manner. The Ad5CMV Cre recombinase adenovirus was purchased from the University of Iowa Gene Transfer Vector Core (Iowa City, IA), and the Ad5CMV LacZ adenovirus was purchased the University of North Carolina Viral Core (Chapel Hill, NC).

Semi-quantitative RT-PCR analysis

Total RNA was isolated from homogenized whole mouse tissues or primary mouse myoblast cultures using RNeasy Mini Kit (Qiagen) according to manufacturer’s instructions. Complimentary DNA (cDNA) was obtained from 1 μg of RNA isolated using the iScript cDNA Synthesis Kit (Bio-Rad,), and PCR amplifications of 30 cycles were performed using 2.5% of total synthesized cDNA and TaKaRa Ex Taq Polymerase (Millipore) according to manufacturer’s instructions using the following primers *graf1* forward 5′-

TGGAAGGGTACCTGTACGTG-3′ and *graf1* reverse 5′-ATCCCG-TTGGTAGGTACAGT-3′, T_a=60 °C; *graf2* forward 5′-TAACAGTCATAT-GAAGATTTTTCGAACCTCGCCTG-3′ and *graf2* reverse 5′-CTGATG-GATCCTTATGCCCGAGCCTTTCGATTGAT-3′, T_a=56 °C (Koeppel et al., 2004); *skeletal alpha actin* forward 5′-CAGAGCAAGCGAGGTATCC-3′ and *skeletal alpha actin* reverse 5′-GTCCCCAGAATCCAACACG-3′, T_a=50 °C; and *gapdh* forward 5′-ATGGGTGTGAACCACGAGAA-3′ and gapdh reverse 5′-GGCATGGACTGTGGTCATGA-3′, T_a=43 °C. RT-PCR products were analyzed by electrophoresis using 2.0% agarose gels.

Cell culture, transfection and siRNA treatment

Primary myoblasts were maintained in growth media (GM; Dulbecco's modified Eagle's medium (DMEM) supplemented with 20% fetal bovine serum (FBS), 10% horse serum (HS) and penicillin/ streptomycin). C2C12 mouse myoblasts obtained from ATCC (Catalog number CRL-1772) were maintained in DMEM supplemented with 10% FBS and antibiotics. C2C12 cells maintained in GM were transfected with Myc-tagged GRAF1 cDNA or GRAF1^{loxp} cDNA using *Trans*IT transfection reagent (Mirus) according to manufacturer's instructions. Myoblasts were infected with Cre- or LacZ-expressing adenoviruses at 100 multiplicities of infection. For differentiation, myoblasts were plated on Lab-Tek CC2 chamber slides or plastic dishes pre-coated with rat tail collagen, Type I (10 μg/ml) and transferred to differentiation medium (DM; DMEM containing 2% HS). In some instances, myoblasts were treated with brefeldin A (Sigma) at indicated concentrations 12 h prior to fixation. GRAF1 and GRAF2 were depleted from cultured myoblasts using short interfering RNA (siRNA) duplex oligoribonucleotides obtained from Invitrogen with the following sequences: *graf1a* sense 5′-GCAGCUGUUGGCCUAUAAU(dT)(dT)-3′ and anti-sense 5′-AUUAUAGGCCAACAGCUGC-3′; *graf1b* sense 5′-AAGUGGACCUG-GUUCGGCAACAUUU-3′ and anti-sense 5′-AAAUGUUGCCGAACCAG-GUCCACUU-3′; and *graf2* sense 5′-CAAAGGUCCAGAGACUUCU-GAGUAU-3′ and anti-sense 5′ -AUACUCAGAAGUCUCUGGAC-CUUUG-3′. Myoblasts maintained in GM or DM were transfected with 150 nM of total gene-specific siRNA (GRAF1 was knocked down using 75 nM of both *graf1*a and *graf1*b, GRAF2 was knocked down using 150 nM of *graf2*, double depletion of GRAF1 and GRAF2 required 37.5 nM each of *graf1*a and *graf1*b and 75 nM of *graf*2, and 150 nM of a GFP-specific siRNA was used as a non-target control (NTC) using DharmaFECT reagent 1 according to manufacturer's instructions (Thermo Scientific)). In some experiments, 50 nM of Block-IT red fluorescent oligonucleotides (Invitrogen) was conco-mitantly transfected with the siRNAs to assess transfection efficiency. After 8 h, media was exchanged and cells were fixed or snap-frozen at indicated time points.

Primary myoblast isolation

Skeletal muscle from GRAF1$^{gt/gt}$ and GRAF1$^{+/+}$ littermates was meticulously isolated from 3–4 P2 neonatal mouse pups per genotype and placed in ice-cold PBS. Once all tissue was harvested, the PBS was exchanged for Hank's Balanced Salt Solution (HBSS; GIBCO) and tissue was transferred to a sterile 100 mm petri dish for mincing using a sterile razor blade in minimal HBSS. Tissue was digested using 0.2% Collagenase, Type II (Worthington

Biochem-icals) in HBSS incubated at 37 °C for 40 min, briefly swirling every 10 min during incubation. Digested muscle was triturated 5 times using a wide-mouth pipette and filtered through a 100 μm nylon mesh cell strainer (BD Biosciences). The cell suspension was then incubated at room temperature for 1 h followed by addition of 30 mL GM and centrifuged at 2000 rpm for 3 min. Cells were pre-plated in GM for 45 min and the remaining suspension was gently transferred to new 100 mm dishes at 1×10^6 cells/dish and incubated undisturbed for 72 h prior to use.

Myoblast differentiation and fusion assays

Myoblasts were seeded at subconfluent densities on collagen-coated slides in GM and after 12 h switched to DM for indicated time. The differentiated index, fusion index, and number of nuclei per field were quantified as described previously, with slight modifications (Jansen and Pavlath, 2006). Briefly, the differentiation index is defined as the ratio of number of nuclei in Tm-positive cells to total number of nuclei counted, while the fusion index is defined as the ratio of number of nuclei in myotubes (≥ 2 nuclei) to total nuclei counted. Images were analyzed using ImageJ software (NIH) to measure the long axis of the cell and cross-sectional cell perimeter.

Immunohistochemistry and immunocytochemistry

Upon harvest, tissues were immediately embedded in Tissue-Tek O.C.T. compound (Sakura), snap-frozen in 2-methylbutane cooled over dry ice, and cross-sectioned at 8 μm using a cryotome. Sections were post-fixed (or cultured myoblasts were fixed) in 4% paraformaldehyde, permeabilized, and stained using standard techniques. The GRAF2, tropomyosin, MHC, Myc-tag, and myoferlin antibodies were diluted at 1:500; The GRAF1, EHD1, EHD2, and Fer1L5 antibodies were diluted at 1:200; The Lamp2 and GM130 antibodies were diluted at 1:100; and the Rab5 antibody was diluted at 1:50. A mouse anti-hamster linker (SouthernBiotech) was used at 1:500 for conjugation to the GRAF1 hamster antibody. Cells/tissues were then incubated with Alexa Fluor secondary antibodies (Invitrogen), Alexa Fluor phalloidin (Invitrogen), Alexa Fluor wheat germ agglutinin (Invitrogen) and DAPI at 1:500 in PBS for 1 h, washed and mounted.

Muscle injury model and in vivo myofiber analysis

Gastrocnemius and diaphragm muscles were harvested from 4 month old $GRAF1^{gt/gt}$ and $GRAF1^{+/+}$ littermates and processed as described previously. To induce muscle injury, 100 μL of 20 μM cardiotoxin *(Naja nigricollis*, Calbiochem) was injected into the gastrocnemius muscle of 4 month old littermates. Muscles were harvested 3, 14 and 28 days post-injury and processed as described. Images were acquired and analyzed using ImageJ software to quantify myofiber cross sectional area. The *in vivo* fusion index was quantified as described previously (Hochreiter-Hufford et al., 2013). Briefly, the *in vivo* fusion index is described as the ratio of number of myofibers with ≥ 2 centrally located nuclear foci to total number of regenerating myofibers.

Fluorescence ratio analysis

The EHD1 fluorescence ratio is defined as the ratio of the EHD1 signal within a pre-fusion complex (10 μm^2 yellow box, Fig. 8f) to the EHD1 signal within the remainder of the cell. Integrated density values obtained using ImageJ were used in the calculation of EHD1 fluorescence ratios. Tm-positive cells which contained 1 or 2 nuclei, and exhibited an elongated phenotype with a prominent pre-fusion complex were imaged using a Zeiss 710 confocal microscope set to a 2 μm pinhole.

Protein isolation, western blotting and co-immunoprecipitation

Tissue samples were snap-frozen in liquid nitrogen, sonicated in modified radioimmune precipitation assay (RIPA) buffer (50 mM HEPES pH 7.2, 0.15 M NaCl, 2 mM EDTA, 0.1% Nonidet P-40, 0.05% sodium deoxycholate, 0.5% Triton X-100 plus 1 mM sodium orthovanadate and 1 × concentrations of both Halt Protease Inhibitor Cocktail (Thermo Scientific) and Halt Phosphatase Inhibitor Cocktail (Thermo Scientific)), and cleared by centrifugation. Cultured C2C12 mouse myoblasts were directly lysed and cleared in RIPA buffer. For immunoprecipitation studies, 1 mg of cleared lysate was incubated with 10 μg of either an anti-GRAF1 antibody (polyclonal) or the corresponding non-immune sera (NIS) overnight at 4 °C. The solution was then mixed with 75 μL of a 50% slurry of Protein A Sepharose beads (Sigma) in TBS and rotated at 4 °C for 2 h. Beads were then quickly tapped down in a refrigerated centrifuge and rinsed 3 times with ice-cold RIPA+inhibitors and once with TBS before beads were boiled in 50 μL of sample buffer. Lysates were resolved by SDS-PAGE, transferred to nitrocellulose membranes, and immunoblotted with antibodies at 1:1000 dilutions using standard techniques.

Microscopy

Cells and tissue sections were examined by confocal microscopy using a Zeiss CLSM 710 Spectral Confocal Laser Scanning Microscope. Confocal Z-stack images were obtained and 3D images were reconstructed using IMARIS software.

Statistical analyses

All statistical analyses were performed using Student's *t*-test. Data are expressed as mean ± s.e.m. and p-values < 0.05 were considered statistically significant. Western blots were performed three separate times with representative images shown. Cellular phenotypes were scored from three independent experiments.

Results

Generation of GRAF1 deficient mice

To explore a role for GRAF1 in promoting myoblast fusion *in vivo*, we generated a GRAF1 deficient mouse line using ES cells that contained an inhibitory gene trap within the first intron of *Graf1* (Fig. 1a). Crosses between $GRAF1^{+/gt}$ mice yielded offspring in the appropriate Mendelian ratios as assessed by validated PCR genotyping (Fig. 1b and Supplementary Table S1). GRAF1 was strongly but not completely depleted in all tissues evaluated indicating that our model results in a hypomorphic allele. Importantly, GRAF1

mRNA levels and protein were virtually undetectable in all skeletal muscle types evaluated (gastrocnemius, quadriceps femoralis, triceps, and diaphragm) supporting the value of this model to further investigate a role for GRAF1 in the development and maintenance of these tissues (Fig. 1c). As previously reported, GRAF1 is also highly expressed in the brain and while a significant reduction in message and protein was observed therein, some residual expression did remain. The tissue-specific differences in residual GRAF1 mRNA levels in the $GRAF1^{gt/gt}$ mice were likely due to the differential expression or activity of splicing factors (Braunschweig et al., 2013).

GRAF1 is necessary to promote proper muscle growth in vivo

No overt phenotypes were observed in $GRAF1^{+/gt}$ or $GRAF1^{gt/gt}$ mice for up to 1 year, though a modest reduction in body weight was observed in young adult homozygous mutant mice (27.2+/−1.0g *versus* 24.3+/−1.6 g; p=0.13 at 4 months of age). To determine if GRAF1 is necessary for efficient muscle growth, we quantified the cross sectional area (CSA) of different muscle types. As shown in Fig. 2, the distribution of fiber size showed a relative lack of large myofibers and more small fibers in $GRAF1^{gt/gt}$ diaphragm and gastrocnemius muscles compared to littermate controls. Concomitantly, mean fiber size of both muscles types were significantly smaller in $GRAF1^{gt/gt}$ mice than in littermate controls. Since myofiber CSA is known to correlate with force production, we next measured the grip force of $GRAF1^{+/+}$ and $GRAF1^{gt/gt}$ mice using a digital strain gauge (Qiao et al., 2008). Confirming an important role for GRAF1 in muscle formation, we found that $GRAF1^{gt/gt}$ mice exhibited a significant reduction in grip strength compared to $GRAF1^{+/+}$ mice (137.9+/−6.2 N *versus* 151.2 +/−6.8N respectively; p<0.05). No significant difference in levels of differentiation markers were observed in P1 or P10 muscles, indicating that the muscle development defect was likely due to impaired muscle fusion, not differentiation (Supplemental Fig. S1a).

Besides its importance in formation of large muscle fibers during development, myoblast fusion plays a key role in the regeneration of injured muscle. To determine if GRAF1 might also function in this setting, we treated Wt mice with cardiotoxin and evaluated GRAF1 expression 3,14, and 28 days later. We found that while GRAF1 was expressed at very low levels in un-injured adult muscle, GRAF1 was transiently increased at early stages of muscle regeneration particularly within the smaller nascent myotubes that were most abundant 3 days following injury. To explore a functional role for GRAF1 in mediating fusion during muscle regeneration, we quantified nuclear accretion and growth in regenerating Wt and $GRAF1^{gt/gt}$ muscles 14 and 28 days post-injury. As shown in Fig. 3b, a significant reduction in the average number of nuclei was observed in regenerating $GRAF^{gt/gt}$ myofibers compared to $GRAF1^{+/+}$ littermates. Moreover, after 14 days, the $GRAF1^{gt/gt}$ mice exhibited a significant reduction in the number of regenerating myofibers with two or more nuclear foci (*in vivo* fusion index) (Fig. 3c and d; Supplemental Fig. S2a). This reduction in nuclear foci persisted to 28 days post-injury and a concomitant significant reduction in the CSA of the regenerating myofibers was observed at this time point (Fig. 3d and e; Supplemental Fig. S2b and c). Importantly, we found no significant difference between these groups (75.9279.67 vs. 80.88±5.77, p=0.33), indicating that the significantly reduced muscle recovery was not likely due to exacerbated injury in this model. Collectively, these data

indicate that GRAF1 is required for optimal fusion and growth of myofibers during development and following injury.

To confirm and extend these findings, we next compared the fusion capabilities of myoblast cultures isolated from the hindlimb muscles of P2 GRAF1$^{gt/gt}$ and GRAF1$^{+/+}$ littermates. Cells were plated at high density and subjected to differentiation media (DM) to induce myotube formation. While no significant difference was observed in the differentiation index (i.e., tropomyosin positive nuclei/total nuclei) or differentiation marker expression (Supplemental Fig. S1b), a significant decrease in the fusion index (*i.e.*, the percentage of nuclei present in multinucleated cells) was observed in GRAF$^{gt/gt}$ compared to GRAF1$^{+/+}$ cultures (Fig. 4a–c). As well, while the cell density (nuclei/area) was not different in these cultures, the number of nuclei in multinucleated cells was lower in tropomyosin-positive GRAF$^{gt/gt}$ cells and a concomitant significant reduction in myotube length was observed (Fig. 4d–f).Collectively, these studies indicate that GRAF1 is necessary for appropriate myoblast fusion.

GRAF1 regulates golgi to plasma membrane vesicle trafficking

We next examined the mechanism by which GRAF1 promotes myoblast fusion using C2C12 cells, which are a well-established multipotent mesenchymal progenitor cell line that undergoes asynchronous but spontaneous differentiation into multinucleated skeletal muscle myotubes when cultured under high confluence in DM (Blau et al., 1985; Yaffe, 1968). In accordance with our previous findings (Doherty et al., 2011), GRAF1 is located in discrete actin-devoid complexes at the tips of differentiated C2C12 myoblasts undergoing end-to-end alignment/fusion (Fig. 5a). Interestingly, these GRAF1-labeled regions are also highly enriched in sub-membranous vesicles as detected by differential interference contrast (DIC) microscopy (Fig. 5b). Moreover, we found that GRAF1 co-localized with the early endosomal marker Rab5 within these pre-fusion complexes but did not co-localize with Lamp2 (a marker for degrading lysosomes), indicating that GRAF1 may be a component and/or regulator of endosomal trafficking. In support of this possibility, we found high levels of GRAF1 in the perinuclear region occupied by the GPI-anchored membrane protein, Thy-1, which is known to recycle from the endosomes through the Golgi apparatus and back to the plasma membrane (Fig. 5c and (Green and Kelly, 1992)).

3-D reconstruction of confocal Z-stacks revealed that GRAF1 enriched regions protruded from the cell surface, and that these protrusions are localized to the precise point of contact between fusing myoblasts (Fig. 6a; Supplemental Fig. S3 and S4 and Supplemental Movie). These findings are consistent with the postulate that GRAF1-laden vesicles are recruited to the plasma membranes of fusing cells and that this process may facilitate cell to cell adhesion/fusion. In support of a role for GRAF1 in promoting vesicle to plasma membrane trafficking, we found that ectopic expression of GRAF1 in rounded, proliferating myoblasts induced membrane protrusions and led to robust surface area expansion, which necessitates additional membrane recruitment ((Doherty et al., 2011); Fig. 6b). This phenotype was significantly attenuated by treatment with Brefeldin A (BFA), a drug that inhibits the translocation of secretory and endocytic recycling vesicles from the Golgi to the cell membrane, indicating that GRAF1 promotes plasma membrane expansion by enhancing/

facilitating vesicle recruitment (Fig. 6b,c). To explore a role for this process in the capacity of GRAF1 to promote myoblast fusion, we utilized our Cre-inducible GRAF1 cDNA variant (termed GRAF1^{loxp}) that contains a GFP reporter gene (Supplemental Fig. S5 and (Doherty et al., 2011)). GRAF^{loxp} transfected C2C12 cells were transferred to DM prior to treatment with either LacZ (control) or Cre adenovirus to induce GRAF1 expression. Eighteen hours later, subsets of LacZ or Cre-infected cells were then treated with BFA and nuclear accretion was assessed 24 h later. As shown in Fig. 6d, GRAF1 expressing cells (in the Cre-treated cultures) exhibited a significant increase in myotube fusion when compared with Lac-Z treated cells that contained the GRAF^{loxp} construct, consistent with our previous findings that GRAF1 promotes cell fusion in pre-differentiated myoblasts (Doherty et al., 2011). Importantly, BFA treatment significantly reversed the profusogenic capacity of GRAF1, indicating that GRAF1 promotes fusion of differentiated myoblasts in a vesicle trafficking-dependent manner.

Supplementary material related to this article can be found online at doi:10.1016/j.ydbio.2014.06.025.

GRAF1 promotes plasma membrane recruitment of the fusogenic proteins EHD1, myoferlin, and Fer1L5

The endocytic recycling proteins EHD1 and EHD2 were recently shown to facilitate myoblast fusion by inducing the release of vesicles from the endocytic recycling compartment and promoting subsequent ‘exocytic’ vesicle merging to the plasma membrane (Cai et al., 2009a; Doherty et al., 2008; Posey et al., 2011a, 2011b). As shown in Fig. 7a, GRAF1 and EHD1 exhibited remarkable co-localization in pre-fusion complexes, while little overlap was observed between GRAF1 and EHD2. This finding is noteworthy, because recent studies indicate that EHD2 is primarily localized to caveolae and unlike depletion of EHD1, depletion of EHD2 does not block endocytic recycling in fibroblasts (Cai et al., 2013). As EHD1 was previously reported to bind avidly to the fusogenic proteins, myoferlin and its family member, Fer1L5, and to promote their transport to the plasma membrane (Doherty et al., 2008; Posey et al., 2011a, 2011b), we next sought to determine if GRAF1 co-associated with these proteins. Indeed, we observed significant co-localization of GRAF1 and myoferlin as well as GRAF1 and Fer1L5 in pre-fusion complexes in isolated myoblasts and in intact muscle (Fig. 7a,b). Moreover, myoferlin and GRAF1 exhibited a strong interaction as assessed by co-immunoprecipitation (Fig. 7c). We next explored our hypothesis that GRAF1 might facilitate the recruitment of these proteins to discrete plasma membrane complexes. Since pre-fusion complexes are more readily observed in C2C12 cells than in primary myoblast cultures (because the latter fuse very rapidly in culture), we treated C2C12 cells with GRAF1 siRNAs (which resulted in a partial reduction of GRAF1 protein; Fig. 7d) and analyzed the localization of Fer1L5, myoferlin and EHD1 in cells following exposure to DM. As shown in Fig. 7e, Fer1L5 was no longer localized to foci at the plasma membrane in GRAF1-deficient cells. Additionally, we observed a significant but incomplete reduction of myoferlin and EHD1 localization to these sub-plasma membrane structures accompanied by an increase in perinuclear vesicular staining (Fig. 7e,f). Taken together, these data indicate that GRAF1 regulates the intracellular trafficking of the fusogenic ferlin proteins to promote membrane coalescence.

Functional cooperation of GRAF proteins in myoblast fusion

Studies detailed above indicate that loss of GRAF1 renders myoblast fusion less efficient but does not prevent myotube formation. Thus we next queried whether other members of the GRAF family might serve a redundant role in this process. In mammals, GRAF1 has two closely related family members, GRAF2 and GRAF3. We recently reported that GRAF3 was not expressed in muscle fibers, but instead was strictly restricted to visceral and vascular smooth muscle cells (Bai et al., 2013). On the other hand all three GRAF2 isoforms (Ren et al., 2001) were expressed in perinatal muscles, in a temporal fashion that mirrored expression of GRAF1, indicating the possibility that GRAF2 might exhibit functional redundancy and potentially compensate for the loss of GRAF1 during myotube formation (Fig. 8b). In support of this possibility, GRAF2 expression was markedly induced upon subjecting C2C12 cells to differentiating conditions (Fig. 8b). Moreover, GRAF2 accumulated into similar peri-nuclear and pre-fusion complexes (Fig. 8b, bottom) where it co-localizes with myoferlin. To further explore a role for GRAF2 in muscle fusion, we depleted GRAF2 from primary $GRAF1^{+/+}$ and $GRAF1^{gt/gt}$ myocytes using validated siRNAs (Fig. 8c). We next subjected these cultures to DM for 48 h and quantified nuclear accretion in tropomyosin positive myoblasts. As shown in Fig. 8d, GRAF2 depletion led to a significant reduction in myoblast-myoblast (bi-nucleated) and myoblast-myotube fusion (≥ nuclei). Notably, the lack in fusion in GRAF2-depleted $GRAF1^{+/+}$ cells was even more pronounced than was observed in myoblasts cultured from $GRAF1^{gt/gt}$ litter-mates. Moreover, the recruitment of EHD1 to the tips of GRAF2 depleted C2C12 cells was markedly reduced in comparison to either control or GRAF1-depleted cells (Fig. 8e,f). However, the depletion of GRAF2 from the $GRAF1^{gt/gt}$ cultures did not result in an additive fusion defect, possibly due to incomplete knock-down of this family member or perhaps because these proteins act together as a functional unit.

Discussion

A clear understanding of the molecular mechanisms that govern myogenesis is important for the future development of therapies directed towards ameliorating muscle wasting that occurs with aging and is exacerbated in muscular dystrophies. We previously showed that the Rho-GTPase-activating protein, GRAF1, was transiently up-regulated during myogenesis, and that forced expression of GRAF1 in pre-differentiated myoblasts promoted robust muscle fusion by a process that required GTPase-activating protein-dependent actin remodeling and BAR-dependent membrane binding or sculpting. Through the use of our novel GRAF1 depleted mice, we now show that GRAF1 is essential for efficient myofiber growth *in vivo*. Post-natal $GRAF1^{gt/gt}$ muscles exhibited a significant and persistent reduction in cross-sectional area and adult muscles had an impaired capacity to regenerate following injury, suggestive of a lack of efficient myoblast fusion. Indeed, we found that myoblasts isolated from GRAF1-depleted mice exhibited impaired myoblast to myoblast and myoblast to myotube fusion. Our mechanistic studies reveal that GRAF1 and its related family member, GRAF2, facilitate myoblast fusion by promoting recruitment of the fusogenic ferlin proteins to the plasma membrane.

It has become clear that myoblast fusion occurs in a multi-step fashion in which actin cytoskeletal dynamics and membrane remodeling play key roles, but questions remain regarding the spatial/temporal regulation of and interrelationship between these processes. Over the past several years, studies have revealed that prior to fusion, differentiated myoblasts assume a bipolar elongated shape that is induced by the interaction of nonmuscle myosin 2 A with actin at the plasma membrane and that these so-called F-actin foci mark the future site of myoblast fusion (Duan and Gallagher, 2009; Peckham, 2008). However, subsequent dissolution of the actin focus is essential for cell-cell fusion as evidenced by the findings in Drosophila that mutations in known actin-remodeling genes such as kette, mbc, and SCAR/WAVE all lead to defective fusion accompanied by enlarged F-actin foci that fail to dissolve (Schafer et al., 2007; Schroter et al., 2004). The small GTPase RhoA has been shown to initiate actin polymerization (Narumiya et al., 1997; Yamana et al., 2006) and we previously showed that recruitment of the Rho-GAP GRAF1 from the peri-nuclear region (its sub-cellular locale in proliferating myoblasts) to the tips of pre-fused bipolar differentiated myoblasts is essential for limiting Rho-dependent actin polymerization at these sites (Doherty et al., 2011). One of the potential functions of localized actin de-polymerization is to facilitate trafficking of intracellular vesicles to the fusion site. Elegant electron microscopy studies in Drosophila myoblasts have shown that vesicles accumulate at juxtaposed inner membranes of fusing cells and that this alignment of vesicles is essential for subsequent membrane merging (Schroter et al., 2004). While the exact nature of these vesicles is not clear, studies from the McNally laboratory and others indicate that endocytic recycling vesicles (regulated by EHD1 and EHD2) are involved and that myoferlin and Fer1L5 are critical fusogenic cargo carried by these vesicles (Doherty et al., 2008; Posey et al., 2011a, 2011b). Indeed, expression of a mutant EHD2 that inhibits endocytic vesicle trafficking led to cytoplasmic sequestration of ferlins and inhibited myoblast fusion.

Ferlins have been proposed to be important for mediating plasma membrane ‘capturing’ of intracellular vesicles, though the precise means by which the subsequent merging of plasma membranes of two cells is not clear (Posey et al., 2011a). Our findings that GRAF1 associates with myoferlin and is co-recruited to the plasma membrane with EHD1-labeled endocytic vesicles indicates that GRAF1 is part of this fusogenic complex. Because GRAF1 functions to accelerate actin de-polymerization, and is necessary for mediating the recruitment of EHD1 and ferlins to the plasma membrane, we favor a model in which GRAF1 may associate with vesicles through its BAR domain and that vesicle-associated GRAF1 facilitates clearing of sub-plasmalemmal actin to aid in vesicle capture. In support of this hypothesis, GRAF1 contains a PS-binding PH domain and PS is known to be exposed on the inner leaflets of injured membranes and the outer leaflets of exocytic vesicles (Gerke et al., 2002). Notably, our 3-D reconstructions of pre-fusion/fusion complexes reveal that the GRAF1-labeled vesicles are located to regions of the cell membrane that protrude outward from the cell body. It is likely that GRAF1 facilitates this outward membrane curvature via interactions of its BAR domain with the inner neck of the membrane protrusion as has been shown for its F-BAR containing Rho-GAP relative, srGAP2 (Suetsugu, 2010). Interestingly, GRAF1 protrusions appear at the point of cell-cell contact of pre-fused cells indicating that these complexes might function to promote adhesion of two apposed myoblasts. At this stage, these protrusive complexes could promote

enhanced hydrophobic attractions between the interiors of the two bilayers, and facilitate lipid transfer from one membrane to another (Chanturiya et al., 2002; Marrink and Mark, 2003). Buckled membranes also exhibit curvature-induced stress and thus can accelerate the fusion process by reducing the energy barrier membranes need to overcome at intermediate stages of fusion (Martens et al., 2007). While our data strongly support a model whereby GRAF1 facilitates membrane merging by promoting the recruitment of ferlin-containing vesicles, numerous cell-surface receptors have been implicated in promoting the initial stages of myoblast fusion including M-cadherin and NCAM that mediate cell recognition and integrins that mediate cell-cell adhesion and it is formally possible that GRAF1-dependent recruitment of these receptors is involved (Simionescu and Pavlath, 2011).

Besides specifying the position of cell-cell fusion and promoting membrane contact, GRAF1 may also play an important role in the late stages of syncytium formation which involves fusion pore expansion to allow complete coalescence of cytoplasms. In this final stage of cell-cell fusion, initial pores of a few nanometers in diameter undergo an active expansion to yield a lumen of 10–15 μm (*i.e.* the diameter of a typical myoblast). The Chernomordik laboratory and others have shown that expansion of such pores that contain strongly bent plasma membrane rims requires persistent energy input and they have postulated that curvature generating proteins that relax the bending energy of the rim are likely required to make expansion energetically favorable (Chernomordik and Kozlov, 2003). BAR domain-containing proteins are likely candidates as these domains form elongated homodimers characterized by a shallow curvature formed by the anti-parallel interaction of two α-helical coils that facilitate membrane deformation (Henne et al., 2007). Previous studies showed that the GRAF1 BAR domain is capable of inducing tubulation of spherical lipids and can promote clathrin-independent endocytosis in fibroblasts and HeLa cells (Eberth et al., 2009; Lundmark et al., 2008). Interestingly, the curvature of the membrane at the fusion pore rim and the curvature of endocytic vesicles are similar, and using an elegant model system to study the efficiency of late stages of cell-cell fusion initiated by influenza and baculoviruses, Richard et al. showed that the GRAF1 BAR domain promoted syncytium formation (Richard et al., 2011). In support of a putative role for GRAF1 in mediating this process during skeletal muscle cell fusion, we found that GRAF1 protein accumulates within the narrow neck that joins two fusing myoblasts (see Fig. 5a for example). Whether GRAF1 serves to stabilize the fusion pore and/or to promote endocytosis-dependent internalization of excess plasma membrane from fusing cells (Kalderon and Gilula, 1979) are interesting questions for future studies.

While the loss of GRAF1 clearly makes myoblast fusion less efficient, muscle development was not completely blocked in GRAF1$^{gt/gt}$ mice. This finding indicates that other proteins are able to compensate for the loss of GRAF1. One attractive candidate is GRAF2, a closely related family member that is widely expressed (Ren et al., 2001). We showed that like GRAF1, mammalian GRAF2 is also highly up-regulated during skeletal muscle maturation, and that GRAF2 depletion significantly attenuated myoblast-myoblast and myoblast-myotube fusion in WT primary muscle cell cultures. Moreover, GRAF2 was localized to similar pre-fusion complexes, and its depletion resulted in a marked reduction of EHD1 and myoferlin accumulation to these sites. These data indicate that these family members may

have functionally overlapping roles during muscle development or may act together as a functional unit. Interestingly, while GRAF1 and GRAF2 exhibit an identical BAR-PH-GAP-SH3 domain structure, they do have a variable serine/proline region which we previously showed is a hot-spot for phosphorylation (Taylor et al., 1998), thus it is possible that these proteins are differentially regulated by kinase signaling pathways. While we did not see evidence of GRAF2 overexpression in isolated GRAF1$^{gt/gt}$ myoblasts when compared to GRAF1$^{+/+}$ cells, we have not ruled out the possibility that transient up-regulation occurs in developing GRAF$^{gt/gt}$ muscles. Other classes of BAR domain containing proteins may also be important for promoting GRAF-independent muscle fusion. For example, two members of the Bridging integrator (Bin) family, Bin1 and Bin3 have been shown to regulate differentiation and fusion of skeletal myoblasts (Fernando et al., 2009; Simionescu-Bankston et al., 2013; Wechsler-Reya et al., 1998). Interestingly, while Bin3 is an N-BAR only containing protein, recent studies indicate that it, like GRAF1, also regulates actin dynamics. Simionescu-Bankston et al. recently showed that Bin3 associates with and promotes the activation of the Rho-related GTPases Cdc42 and Rac1 in myoblasts (Simionescu-Bankston et al., 2013). Notably, activation of these GTPases is often associated with an inhibition of RhoA; however the effect of Bin3 on RhoA activity was not directly tested in this model. It will be of interest to determine whether the Bin proteins also exhibit some functional overlap with the GRAF proteins or are co-regulated through putative BAR domain heterodimerization as has been observed in other BAR family members.

In summary, we provide the first evidence that GRAF1 plays an important role in muscle formation *in vivo*. The phenotype of the GRAF1$^{gt/gt}$ mice resembles myoferlin-null mice (Doherty et al., 2005) and our mechanistic studies reveal that GRAF1 co-associates with ferlins and regulates the recruitment of these fusogenic proteins to the plasma membrane. This study furthers our understanding of the inter-relationship between cytoskeletal and membrane dynamics during myotube formation.

Supplementary Material

Refer to Web version on PubMed Central for supplementary material.

Acknowledgments

This work was supported by Grants from the National Heart, Lung, and Blood Institute, National Institutes of Health (HL-081844 and HL-071054 to J.M. Taylor) and the Muscular Dystrophy Association (MDA255577) to J.M. Taylor. K.C. Lenhart was supported by the National Institutes of Health, USA (T32 HD046369-05 and T32 HL069768-09).

Appendix A. Supporting information

Supplementary data associated with this article can be found in the online version at http://dx.doi.org/10.1016/j.ydbio.2014.06.025.

References

Bai X, Lenhart KC, Bird KE, Suen AA, Rojas M, Kakoki M, Li F, Smithies O, Mack CP, Taylor JM. The smooth muscle-selective RhoGAP GRAF3 is a critical regulator of vascular tone and hypertension. Nat Commun. 2013; 4:2910. [PubMed: 24335996]

Bansal D, Miyake K, Vogel SS, Groh S, Chen CC, Williamson R, McNeil PL, Campbell KP. Defective membrane repair in dysferlin-deficient muscular dystrophy. Nature. 2003; 423:168–172. [PubMed: 12736685]

Blau HM, Chiu CP, Pavlath GK, Webster C. Muscle gene expression in heterokaryons. Adv Exp Med Biol. 1985; 182:231–247. [PubMed: 4003160]

Braunschweig U, Gueroussov S, Plocik AM, Graveley BR, Blencowe BJ. Dynamic integration of splicing within gene regulatory pathways. Cell. 2013; 152:1252–1269. [PubMed: 23498935]

Cai B, Giridharan SS, Zhang J, Saxena S, Bahl K, Schmidt JA, Sorgen PL, Guo W, Naslavsky N, Caplan S. Differential roles of C-terminal Eps15 homology domain proteins as vesiculators and tubulators of recycling endosomes. J Biol Chem. 2013; 288:30172–30180. [PubMed: 24019528]

Cai C, Masumiya H, Weisleder N, Pan Z, Nishi M, Komazaki S, Takeshima H, Ma J. MG53 regulates membrane budding and exocytosis in muscle cells. J Biol Chem. 2009a; 284:3314–3322. [PubMed: 19029292]

Cai C, Weisleder N, Ko JK, Komazaki S, Sunada Y, Nishi M, Takeshima H, Ma J. Membrane repair defects in muscular dystrophy are linked to altered interaction between MG53, caveolin-3, and dysferlin. J Biol Chem. 2009b; 284:15894–15902. [PubMed: 19380584]

Chanturiya A, Scaria P, Kuksenok O, Woodle MC. Probing the mechanism of fusion in a two-dimensional computer simulation. Biophys J. 2002; 82:3072–3080. [PubMed: 12023230]

Chernomordik LV, Kozlov MM. Protein-lipid interplay in fusion and fission of biological membranes. Annu Rev Biochem. 2003; 72:175–207. [PubMed: 14527322]

DiMichele LA, Hakim ZS, Sayers RL, Rojas M, Schwartz RJ, Mack CP, Taylor JM. Transient expression of FRNK reveals stage-specific requirement for focal adhesion kinase activity in cardiac growth. Circ Res. 2009; 104:1201–1208. [PubMed: 19372463]

Doherty JT, Lenhart KC, Cameron MV, Mack CP, Conlon FL, Taylor JM. Skeletal muscle differentiation and fusion are regulated by the BAR-containing Rho-GTPase-activating protein (Rho-GAP), GRAF1. J Biol Chem. 2011; 286:25903–25921. [PubMed: 21622574]

Doherty KR, Cave A, Davis DB, Delmonte AJ, Posey A, Earley JU, Hadhazy M, McNally EM. Normal myoblast fusion requires myoferlin. Development. 2005; 132:5565–5575. [PubMed: 16280346]

Doherty KR, Demonbreun AR, Wallace GQ, Cave A, Posey AD, Heretis K, Pytel P, McNally EM. The endocytic recycling protein EHD2 interacts with myoferlin to regulate myoblast fusion. J Biol Chem. 2008; 283:20252–20260. [PubMed: 18502764]

Duan R, Gallagher PJ. Dependence of myoblast fusion on a cortical actin wall and nonmuscle myosin IIA. Dev Biol. 2009; 325:374–385. [PubMed: 19027000]

Eberth A, Lundmark R, Gremer L, Dvorsky R, Koessmeier KT, McMahon HT, Ahmadian MR. A BAR domain-mediated autoinhibitory mechanism for RhoGAPs of the GRAF family. Biochem J. 2009; 417:371–377. [PubMed: 18954304]

Evesson FJ, Peat RA, Lek A, Brilot F, Lo HP, Dale RC, Parton RG, North KN, Cooper ST. Reduced plasma membrane expression of dysferlin mutants is attributed to accelerated endocytosis via a syntaxin-4-associated pathway. J Biol Chem. 2010; 285:28529–28539. [PubMed: 20595382]

Fernando P, Sandoz JS, Ding W, Repentigny Y, Brunette S, Kelly JF, Kothary R, Megeney LA. Bin1 SRC homology 3 domain acts as a scaffold for myofiber sarcomere assembly. J Biol Chem. 2009; 284:27674–27686. [PubMed: 19633357]

Gerke V, Moss SE. Annexins: from structure to function. Physiol Rev. 2002; 82:331–371. [PubMed: 11917092]

Green SA, Kelly RB. Low density lipoprotein receptor and cation-independent mannose 6-phosphate receptor are transported from the cell surface to the Golgi apparatus at equal rates in PC12 cells. J Cell Biol. 1992; 117:47–55. [PubMed: 1313438]

Han R, Bansal D, Miyake K, Muniz VP, Weiss RM, McNeil PL, Campbell KP. Dysferlin-mediated membrane repair protects the heart from stress-induced left ventricular injury. J Clin Invest. 2007; 117:1805–1813. [PubMed: 17607357]

Henne WM, Kent HM, Ford MG, Hegde BG, Daumke O, Butler PJ, Mittal R, Langen R, Evans PR, McMahon HT. Structure and analysis of FCHo2 F-BAR domain: a dimerizing and membrane

recruitment module that effects membrane curvature. Structure. 2007; 15:839–852. [PubMed: 17540576]

Hildebrand JD, Taylor JM, Parsons JT. An SH3 domain-containing GTPase-activating protein for Rho and Cdc42 associates with focal adhesion kinase. Mol Cell Biol. 1996; 16:3169–3178. [PubMed: 8649427]

Hochreiter-Hufford AE, Lee CS, Kinchen JM, Sokolowski JD, Arandjelovic S, Call JA, Klibanov AL, Yan Z, Mandell JW, Ravichandran KS. Phosphatidylserine receptor BAI1 and apoptotic cells as new promoters of myoblast fusion. Nature. 2013; 497:263–267. [PubMed: 23615608]

Jansen KM, Pavlath GK. Mannose receptor regulates myoblast motility and muscle growth. J Cell Biol. 2006; 174:403–413. [PubMed: 16864654]

Kalderon N, Gilula NB. Membrane events involved in myoblast fusion. J Cell Biol. 1979; 81:411–425. [PubMed: 468911]

Koeppel MA, McCarthy CC, Moertl E, Jakobi R. Identification and characterization of PS-GAP as a novel regulator of caspase-activated PAK-2. J Biol Chem. 2004; 279:53653–53664. [PubMed: 15471851]

Lundmark R, Doherty GJ, Howes MT, Cortese K, Vallis Y, Parton RG, McMahon HT. The GTPase-activating protein GRAF1 regulates the CLIC/GEEC endocytic pathway. Curr Biol. 2008; 18:1802–1808. [PubMed: 19036340]

Marrink SJ, Mark AE. The mechanism of vesicle fusion as revealed by molecular dynamics simulations. J Am Chem Soc. 2003; 125:11144–11145. [PubMed: 16220905]

Martens S, Kozlov MM, McMahon HT. How synaptotagmin promotes membrane fusion. Sci. 2007; 316:1205–1208.

Matsuda C, Hayashi YK, Ogawa M, Aoki M, Murayama K, Nishino I, Nonaka I, Arahata K, Brown RH Jr. The sarcolemmal proteins dysferlin and caveolin-3 interact in skeletal muscle. Hum Mol Genet. 2001; 10:1761–1766. [PubMed: 11532985]

Narumiya S, Ishizaki T, Watanabe N. Rho effectors and reorganization of actin cytoskeleton. FEBS Lett. 1997; 410:68–72. [PubMed: 9247125]

Peckham M. Engineering a multi-nucleated myotube, the role of the actin cytoskeleton. J Microsc. 2008; 231:486–493. [PubMed: 18755004]

Posey AD Jr, Demonbreun A, McNally EM. Ferlin proteins in myoblast fusion and muscle growth. Curr Top Dev Biol. 2011a; 96:203–230. [PubMed: 21621072]

Posey AD Jr, Pytel P, Gardikiotes K, Demonbreun AR, Rainey M, George M, Band H, McNally EM. Endocytic Recycling Proteins EHD1 and EHD2 Interact with Fer-1-like-5 (Fer1L5) and Mediate Myoblast Fusion. J Biol Chem. 2011b; 286:7379–7388. [PubMed: 21177873]

Qiao C, Li J, Jiang J, Zhu X, Wang B, Li J, Xiao X. Myostatin propeptide gene delivery by adeno-associated virus serotype 8 vectors enhances muscle growth and ameliorates dystrophic phenotypes in mdx mice. Hum Gene Ther. 2008; 19:241–254. [PubMed: 18288893]

Ren XR, Du QS, Huang YZ, Ao SZ, Mei L, Xiong WC. Regulation of CDC42 GTPase by proline-rich tyrosine kinase 2 interacting with PSGAP, a novel pleckstrin homology and Src homology 3 domain containing rhoGAP protein. J Cell Biol. 2001; 152:971–984. [PubMed: 11238453]

Richard JP, Leikina E, Langen R, Henne WM, Popova M, Balla T, McMahon HT, Kozlov MM, Chernomordik LV. Intracellular curvature-generating proteins in cell-to-cell fusion. Biochem J. 2011; 440:185–193. [PubMed: 21895608]

Schafer G, Weber S, Holz A, Bogdan S, Schumacher S, Muller A, Renkawitz-Pohl R, Onel SF. The Wiskott-Aldrich syndrome protein (WASP) is essential for myoblast fusion in Drosophila. Dev Biol. 2007; 304:664–674. [PubMed: 17306790]

Schroter RH, Lier S, Holz A, Bogdan S, Klambt C, Beck L, Renkawitz-Pohl R. kette and blown fuse interact genetically during the second fusion step of myogenesis in Drosophila. Dev. 2004; 131:4501–4509.

Simionescu-Bankston A, Leoni G, Wang Y, Pham PP, Ramalingam A, DuHad-away JB, Faundez V, Nusrat A, Prendergast GC, Pavlath GK. The N-BAR domain protein, Bin3, regulates Rac1- and Cdc42-dependent processes in myogenesis. Dev Biol. 2013; 382:160–171. [PubMed: 23872330]

Simionescu A, Pavlath GK. Molecular mechanisms of myoblast fusion across species. Adv Exp Med Biol. 2011; 713:113–135. [PubMed: 21432017]

Suetsugu S. The proposed functions of membrane curvatures mediated by the BAR domain superfamily proteins. J Biochem. 2010; 148:1–12. [PubMed: 20435640]

Swailes NT, Knight PJ, Peckham M. Actin filament organization in aligned prefusion myoblasts. J Anat. 2004; 205:381–391. [PubMed: 15575887]

Taylor JM, Hildebrand JD, Mack CP, Cox ME, Parsons JT. Characterization of graf, the GTPase-activating protein for rho associated with focal adhesion kinase. Phosphorylation and possible regulation by mitogen-activated protein kinase. J Biol Chem. 1998; 273:8063–8070. [PubMed: 9525907]

Taylor JM, Macklem MM, Parsons JT. Cytoskeletal changes induced by GRAF, the GTPase regulator associated with focal adhesion kinase, are mediated by Rho. J Cell Sci. 1999; 112(Pt 2):231–242. [PubMed: 9858476]

Wallace GQ, McNally EM. Mechanisms of muscle degeneration, regeneration, and repair in the muscular dystrophies. Annu Rev Physiol. 2009; 71:37–57. [PubMed: 18808326]

Wechsler-Reya RJ, Elliott KJ, Prendergast GC. A role for the putative tumor suppressor Bin1 in muscle cell differentiation. Mol Cell Biol. 1998; 18:566–575. [PubMed: 9418903]

Yaffe D. Retention of differentiation potentialities during prolonged cultivation of myogenic cells. Proc Natl Acad Sci U S A. 1968; 61:477–483. [PubMed: 5245982]

Yamana N, Arakawa Y, Nishino T, Kurokawa K, Tanji M, Itoh RE, Monypenny J, Ishizaki T, Bito H, Nozaki K, Hashimoto N, Matsuda M, Narumiya S. The Rho-mDia1 pathway regulates cell polarity and focal adhesion turnover in migrating cells through mobilizing Apc and c-Src. Mol Cell Biol. 2006; 26:6844–6858. [PubMed: 16943426]

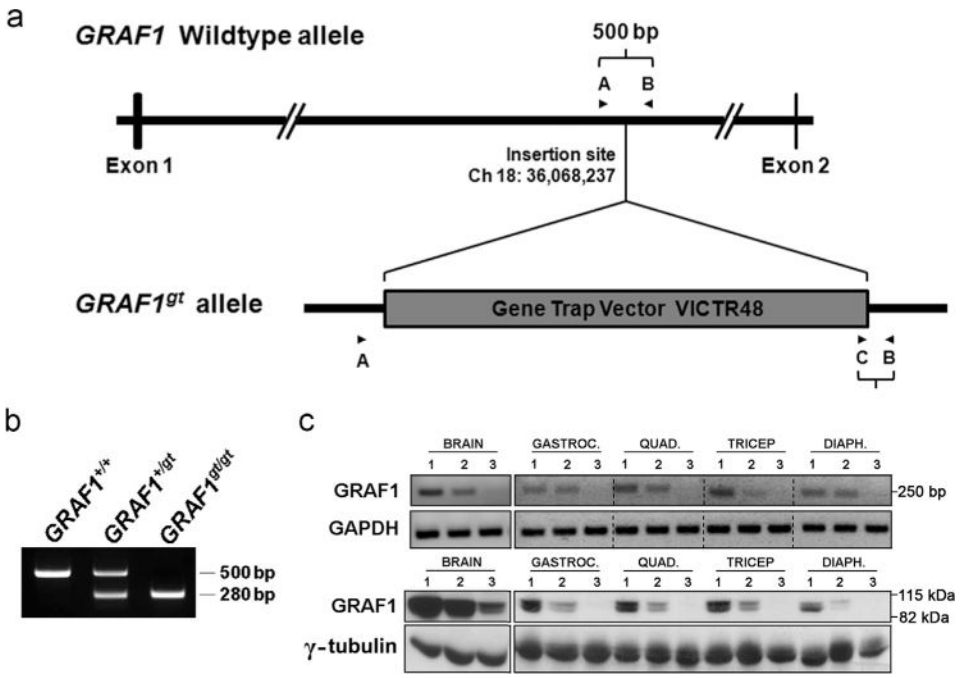

Fig. 1.

Gene trap insertion at the *Graf1* locus disrupts gene expression. (a) The gene trap vector VICTR48 integrated into the first intron of the mouse *Graf1* gene. Arrowheads indicate primer annealing sites for genotype analysis. (b) PCR-based genotyping of isolated tail DNA differentiate wildtype ($GRAF1^{+/+}$) and homozygous mutant ($GRAF1^{gt/gt}$) animals by generating fragments of 500 and 280 bp, respectively. DNA from heterozygotes ($GRAF1^{+/gt}$) generates both fragments. (c) RT-PCR analysis (*top*) of GRAF1 cDNA and Western blot analysis (*bottom*) of GRAF1 protein from P7 pups confirm reduced expression of GRAF1 in heterozygous (2), and homozygous (3) mutant animals relative to wildtype littermates (1). GAPDH (cDNA) and γ-tubulin (protein) were used as loading controls. Gastroc.=Gastrocnemius; Quad.=Quadriceps femoris; and Diaph.= Diaphragm.

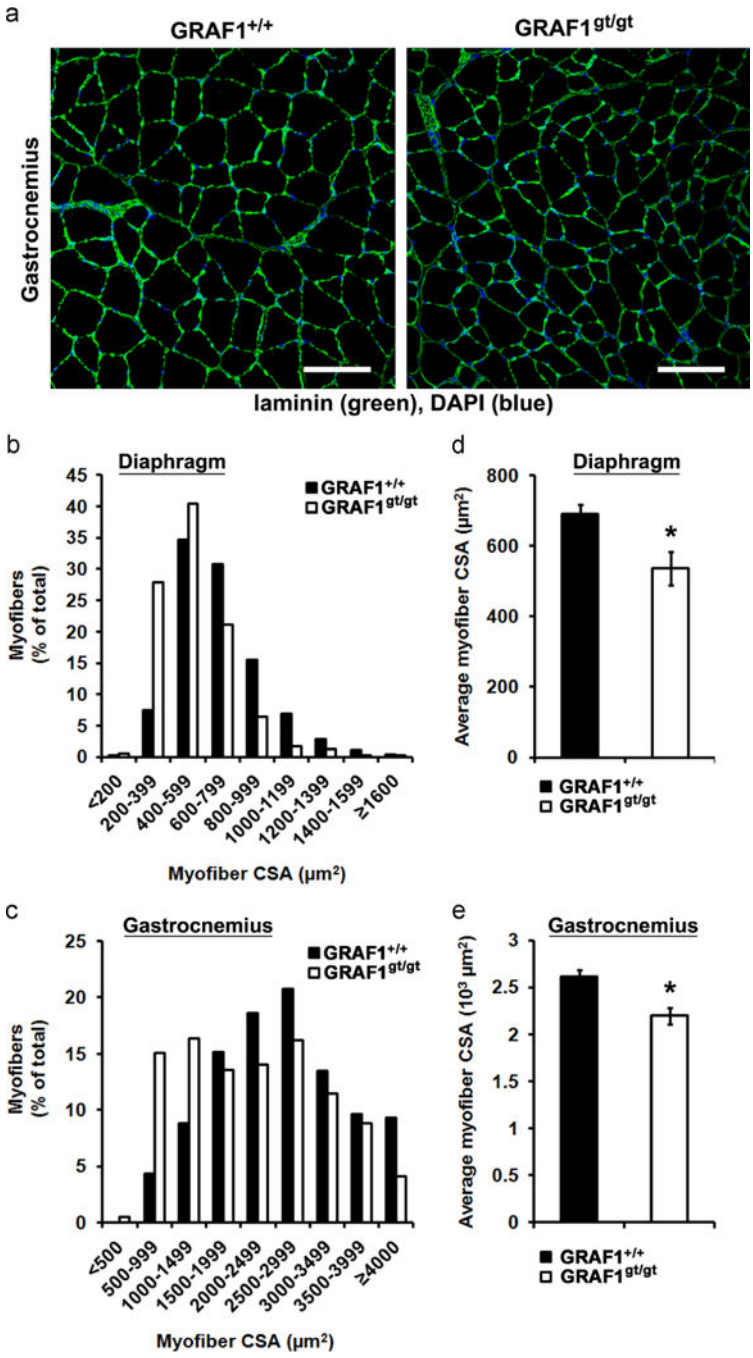

Fig. 2.

GRAF1 regulates myofiber growth *in vivo*. (a) Gastrocnemius muscle from 4 month old GRAF1$^{gt/gt}$ mice exhibit smaller myofibers than GRAF1$^{+/+}$ mice. Laminin (green) demarcates myofiber boundaries. Nuclei are counterstained with DAPI (blue). (b, c) Frequency histograms of myofiber cross-sectional area (CSA) of diaphragm and gastrocnemius muscle from 4 month old GRAF1$^{+/+}$ and GRAF1$^{gt/gt}$ mice. (d, e) Average myofiber CSA of diaphragm and gastrocnemius muscle (*p<0.05; n=350 myofibers per mouse, N=5 mice per genotype). Data are mean±s.e.m. Scale bars=100 μm.

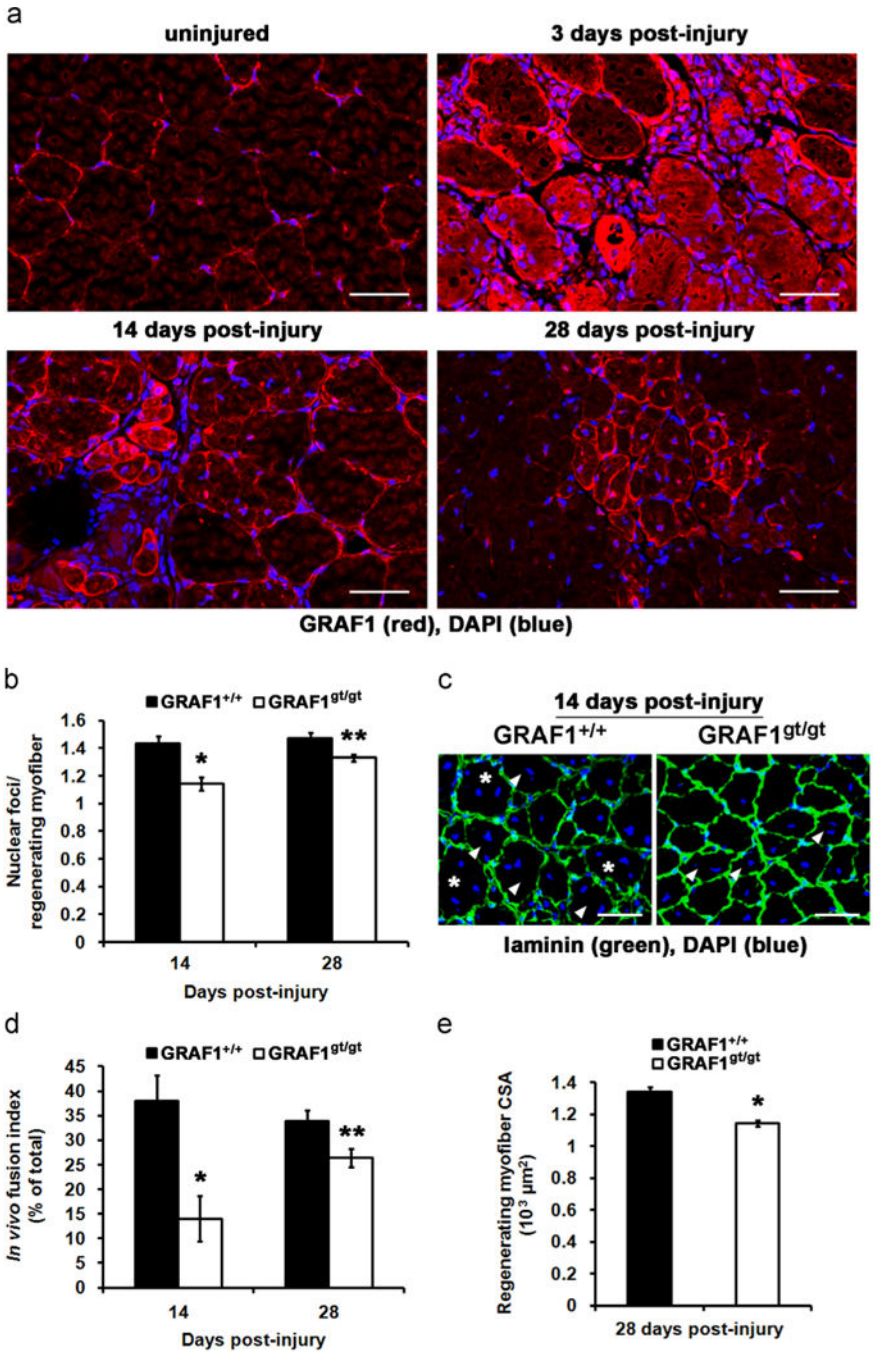

Fig. 3.

GRAF1$^{gt/gt}$ muscles exhibit impaired regenerative capacity (a) Immunohistochemical analysis of GRAF1 expression (red) in uninjured adult gastrocnemius muscle or muscles 3, 14, and 28 days following cardiotoxin-injection. Nuclei are stained with DAPI (blue). (b) Quantification of average nuclear foci per regenerating myofiber 14 and 28 days following cardiotoxin injection (*p<0.005, **p<0.05; n=250 and n=500 myofibers per mouse at 14 and 28 days-post injury, respectively; N=3–5 mice per genotype). (c) Regenerating gastrocnemius muscle from GRAF1$^{gt/gt}$ mice (14 days following cardiotoxin-induced

injury) display fewer regenerating myofibers with 2 (*arrowheads*) or 3 (*asterisks*) nuclear foci than injured GRAF1$^{+/+}$ muscles. Laminin (green) demarcates myofiber boundaries. Nuclei are stained with DAPI (blue). Scale bars=20 μm (d) Quantification of the *in vivo* fusion index for regenerating myofibers 14 and 28 days-post injury (*p<0.005, **p<0.05; n=250 and n=500 myofibers per mouse at 14 and 28 days-post injury, respectively; N=3–5 mice per genotype). (e) Average CSA of regenerating myofibers 28 days post-injury (*p<0.05; n=350 myofibers per mouse, N=3–4 mice per genotype). Data are expressed as mean7s.e.m. Scale bars=100 μM, unless otherwise indicated.

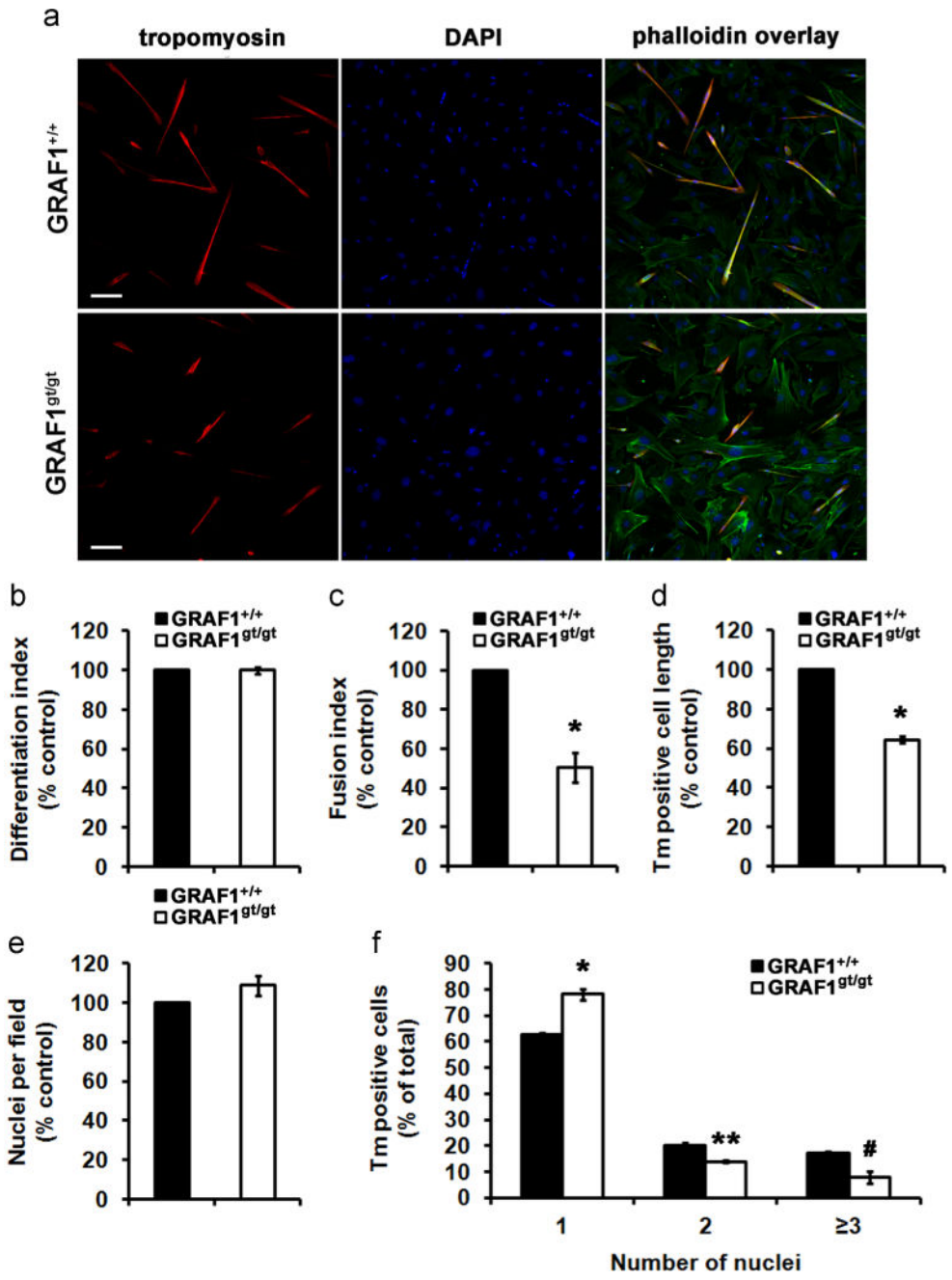

Fig. 4.

GRAF1-depleted myoblast exhibit reduced fusogenic capacity. (a) Representative images of GRAF1$^{+/+}$ and GRAF1$^{gt/gt}$ primary cultures immunostained for tropomyosin (red) at 72 h in differentiation media (DM). F-actin and nuclei are counterstained with phalloidin (green) and DAPI (blue), respectively. (b) GRAF1$^{+/+}$ and GRAF1$^{gt/gt}$ cells immunostained in (4a) exhibited no significant difference in their differentiation index (average index for control was 10.5%). Also see Supplemental Fig. S1b for comparison of skeletal α-actin expression. (c) GRAF1$^{gt/gt}$ cells exhibited a significant decrease in their fusion index (*p<0.005). (d) Tm-positive GRAF1$^{+/+}$ cells were significantly longer than Tm-positive GRAF1$^{gt/gt}$ cells

(*$p<5 \times 10^{-4}$). (e) The number of nuclei per field was comparable between $GRAF1^{+/+}$ and $GRAF1^{gt/gt}$ cultures. (f) $GRAF1^{gt/gt}$ cells exhibited reduced nuclear accretion with a significant increase in mononucleated cells (*$p < 0.005$) and decrease in bi-nucleated (**$p < 0.01$) and multinucleated ($^{\#}p < 0.05$) cells in comparison to $GRAF1^{+/+}$ controls. At least 1000 Tm-positive cells, 250 myotubes, and 10,000 nuclei were scored over 50 images per genotype for each assay. Average fusion index for control cells was 1.2%. Data are mean ± s.e.m., $N=3$ independent experiments. Scale bars =100 μm.

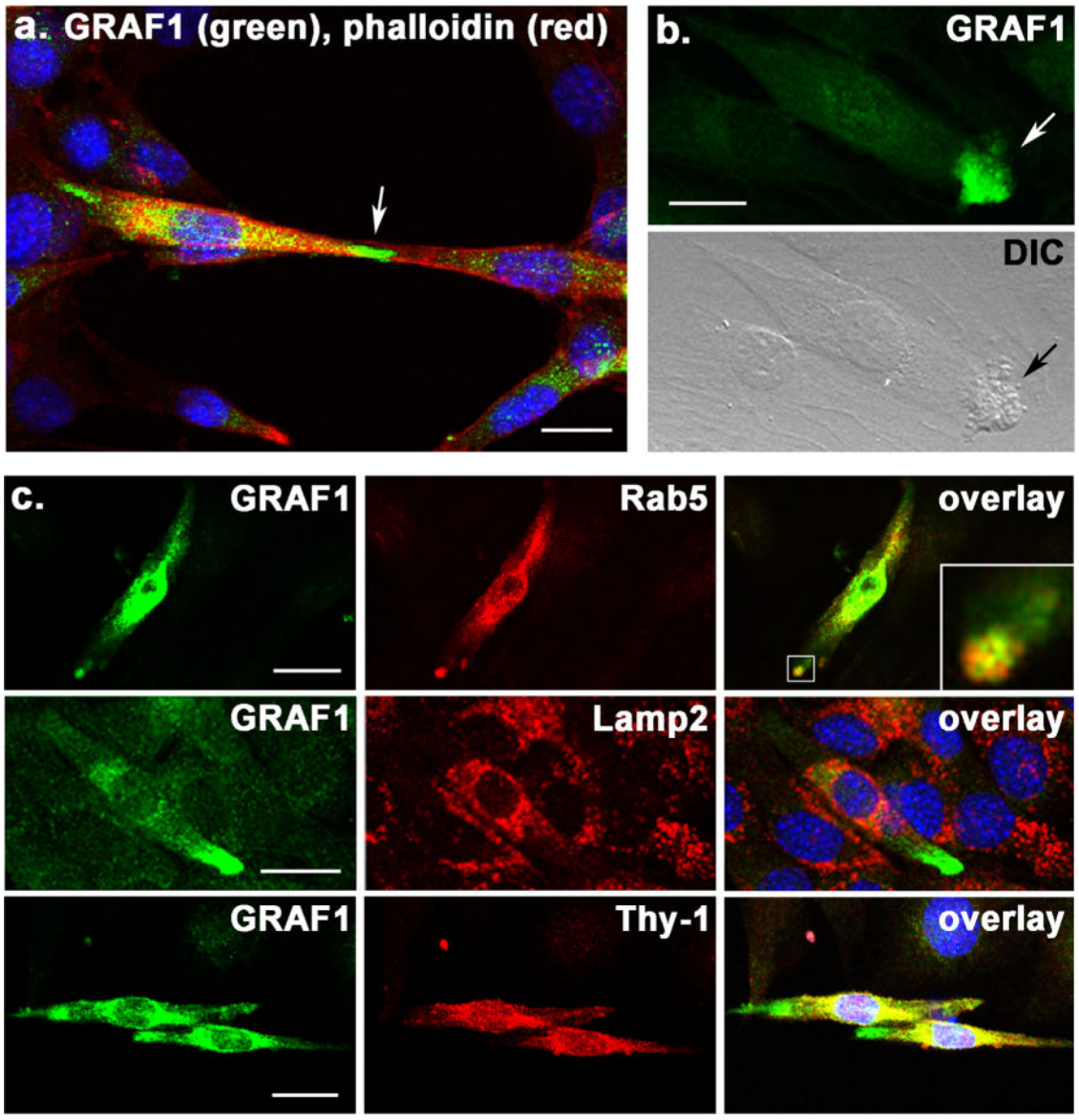

Fig. 5.

GRAF1 is present within endocytic structures in pre-fused myoblasts. (a) Endogenous GRAF1 selectively accumulated within the cytoplasmic bridge (*white arrow*) between actively fusing C2C12 myoblasts. (b) GRAF1 co-localizes with intracellular vesicles (*arrows*) as visualized by DIC microscopy in 48 h differentiated C2C12 myoblasts. (c) Membrane-associated GRAF1 co-localizes with the early endosomal marker Rab5 (*top*), but not with Lamp2-positive lysosomes (*middle*). Perinuclear GRAF1 co-localizes with the endocytic recycling protein Thy-1 (*bottom*). Nuclei are counterstained with DAPI (blue). Scale bars=20 μm.

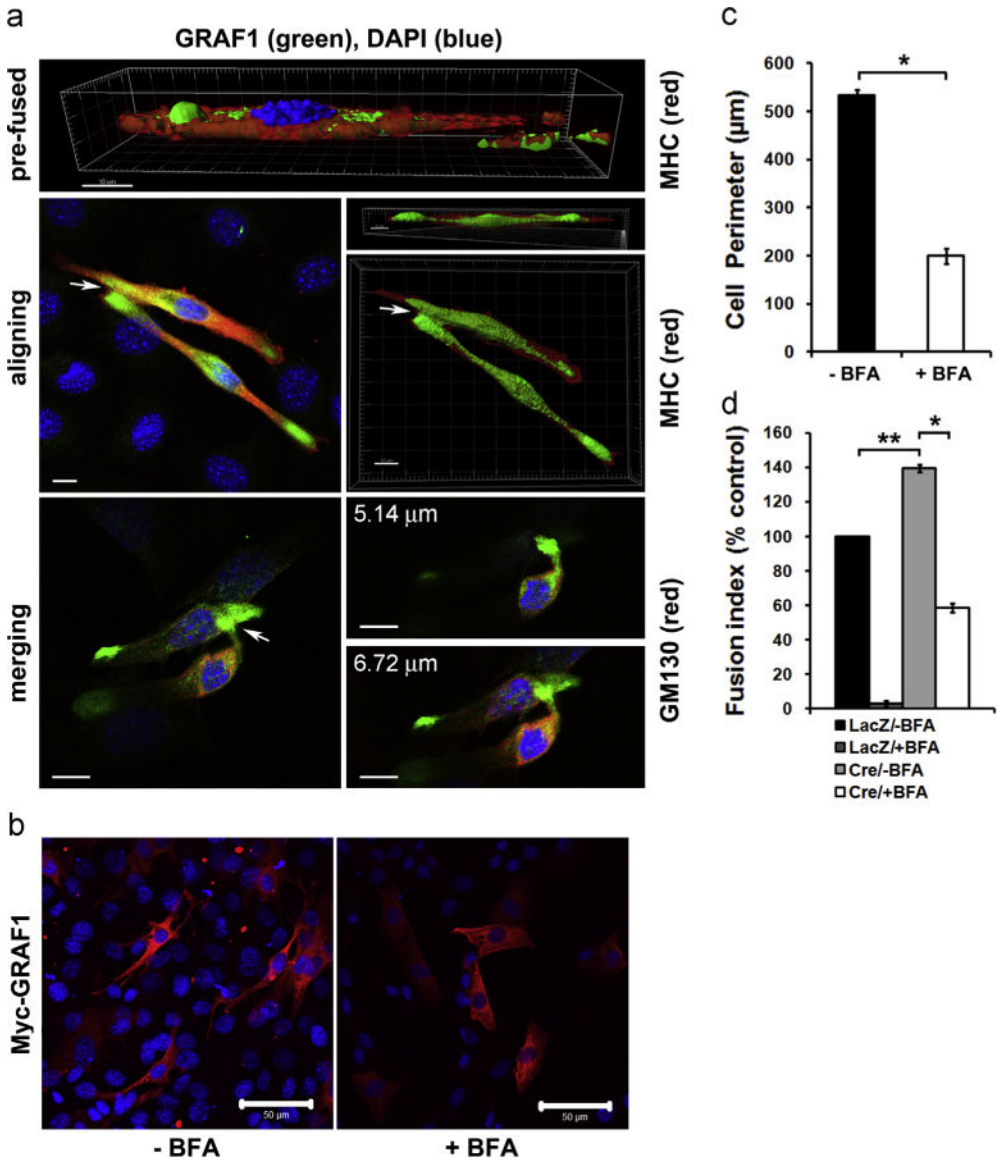

Fig. 6.

GRAF1-dependent membrane protrusions and myoblast fusion is dependent on vesicular trafficking. (a) C2C12 cells were treated with DM for 49–72 h, stained for endogenous GRAF1 (and other indicated antibodies), and visualized by confocal microscopy. Confocal slice views and digital decovolution and 3-D renderings are shown. GRAF1 is localized to complexes that protrude from cells at pre-fusion complexes (*top*, also see Supplemental Fig. S2 for confocal slice view) and at the points of cell-cell contact (*middle*, *white arrows*) as demonstrated using image deconvolution of confocal Z-stacks. GRAF1 is localized to the precise point of contact between fusing myoblasts (*bottom*, *white arrow*), note high levels of GRAF1 accumulation in the protrusion of a myoblast that appears to be diving into a GRAF1-labeled region of a myotube. See Supplemental Fig. S3 for the gallery view of confocal slices of this 6.71 µm maximum intensity projection (MIP). Myosin heavy chain (MHC) demarcates cell boundaries in top and middle panels. GM130 demarcates Golgi

bodies in bottom panel. (b) Representative images of C2C12 cells maintained in growth media and transfected with Myc-tagged GRAF1 for 24 h. Twelve hr prior to fixation, cells were treated with (*right*) or without (*left*) 0.1 μg/mL Brefeldin A (BFA). Anti-Myc (red) identifies GRAF1 overexpressing cells. Nuclei are counterstained with DAPI (blue). Scale bars=50 μm. (c) Quantification of the perimeter of cells represented in Fig. 5b demonstrates significant reduction in the plasma membrane surface area of BFA-treated myoblasts ($^{*}p < 1 \times 10^{-4}$). (d) C2C12 cells were transfected with a Cre recombinase-inducible Myc-tagged GRAF1 targeting construct, induced to differentiate for 48 h in DM, and transduced with Cre or control LacZ adenovirus for 36 h. Twenty four hour prior to fixation, cells were treated with 0.3 μg/mL BFA. Dual Myc and DAPI staining were used to quantify the fusion index ($^{*}p < 1 \times 10^{-4}$, $^{**}p < 0.005$). Average fusion index for control was 6.5%. Data are mean ± s. e.m., n = 75–100 cells per condition, N=3 independent experiments. Scale bars=10 μm, unless otherwise indicated.

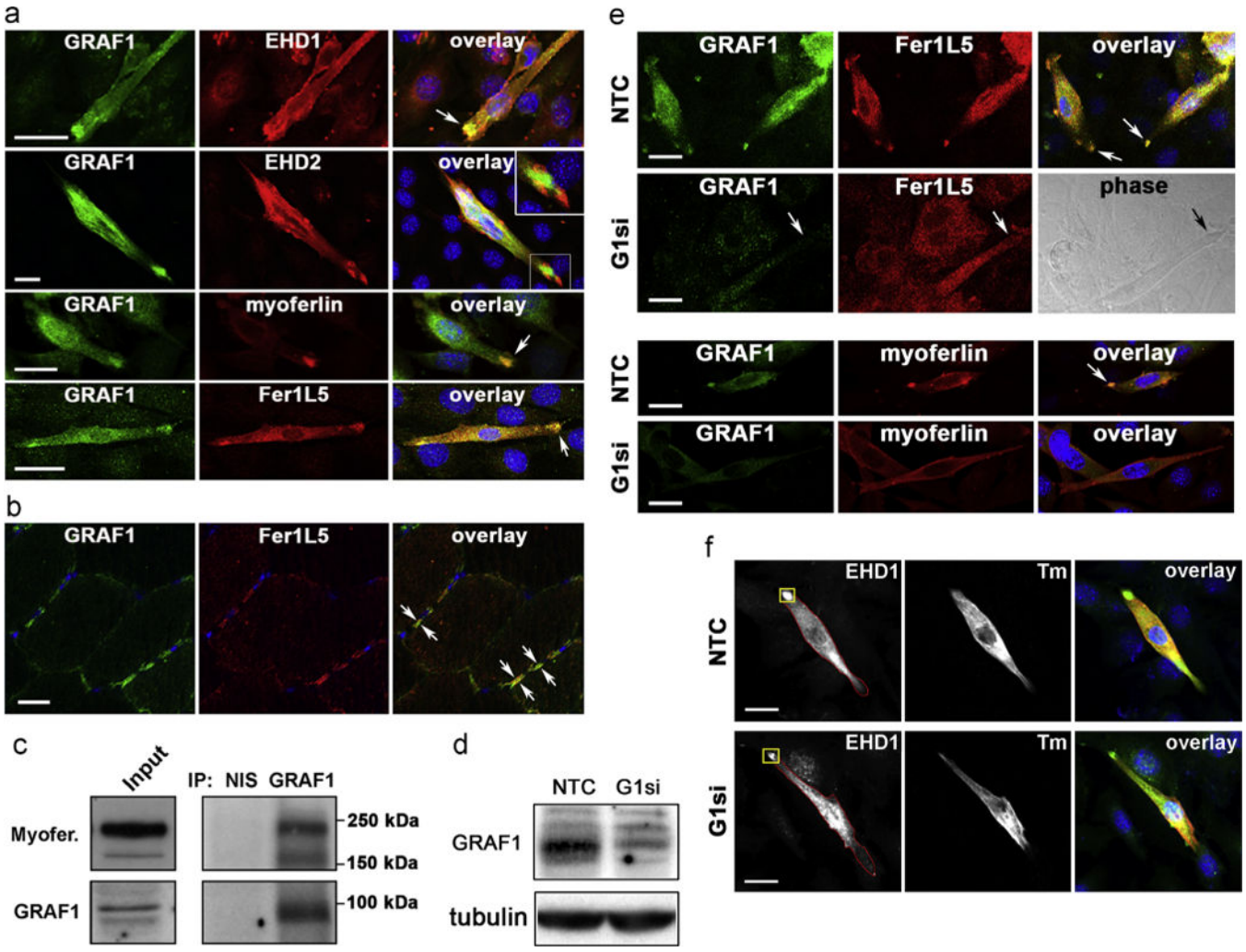

Fig. 7.

GRAF1 associates with the fusogenic ferlin proteins and promotes recruitment of the endocytic recycling machinery to pre-fusion complexes. (a) C2C12 cells exposed to DM for 36 h were co-immunostained with GRAF1 and EHD1 (*top*), EHD2 (*top middle*), myoferlin (bottom middle) or Fer1L5 (*bottom*) antibodies. White arrows indicate co-localization of proteins at pre-fusion sites. High power inset reveals limited co-localization of GRAF1 and EHD2. (b) Tibialis anterior muscle cryo-sections from a 6 month old wildtype mouse were co-stained with GRAF1 and Fer1L5 antibodies (note sarcolemmal co-localization). (c) Anti-GRAF1 rabbit polyclonal antibody and non-immune sera (NIS) immunoprecipitations (IP) from C2C12 cells exposed to DM for 72 h. Blots were probed with an anti-myoferlin antibody or hamster anti-GRAF1 antibody. Input contains 20% of cellular lysate used for IP. (d) C2C12 cells transfected with GRAF1-specific (G1si) or control (NTC) siRNA and exposed to DM for 36 h were lysed and immunoblotted with GRAF1 antibody to assess knockdown efficiency. γ-tubulin is shown as a loading control. (e) C2C12 cells treated as in Fig. 6d were co-stained with GRAF1 and either Fer1L5 or myoferlin antibodies. GRAF1 and ferlin co-localize at polarized tips in NTC treated cells (arrows), and both Fer1L5 and myoferlin are mis-localized in GRAF1 knockdown cells. (f) C2C12 cells treated as in Fig.

6d were co-stained with EHD1 and Tm antibodies to demarcate differentiated myoblasts. Images illustrate the method of quantifying EHD1 protein at pre-fusion complexes. ImageJ software was used to measure the intensity of EHD1 signal at a pre-fusion complex (yellow box) relative to the signal within the rest of the cell. Refer to Fig. 8f for quantification. Data are representative of at least 100 cells/condition. Scale bars=20 μm.

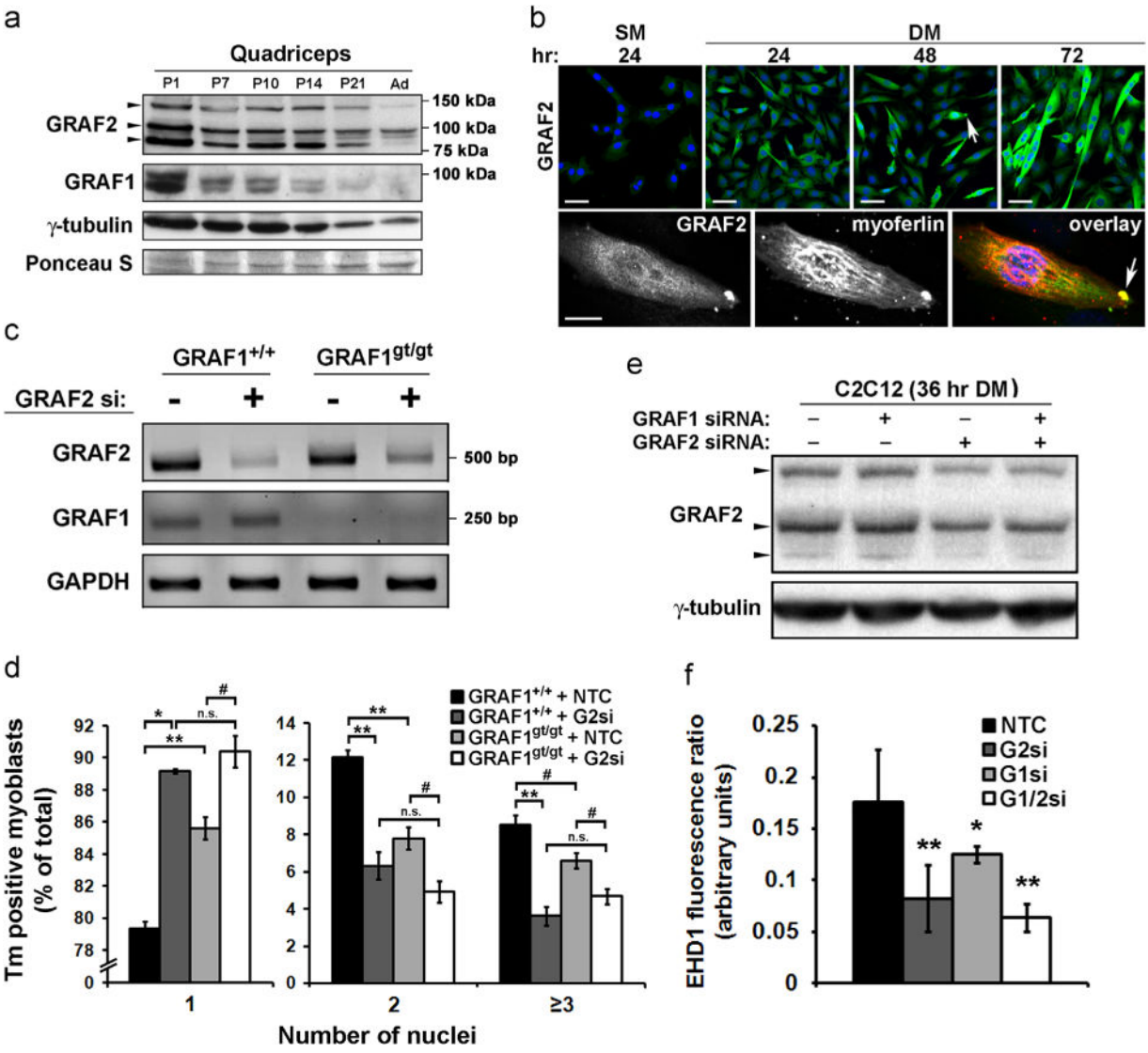

Fig. 8.

GRAF2 also promotes recruitment of the endocytic recycling machinery to pre-fusion complexes and muscle fusion. (a) Western blot analysis of GRAF1 and GRAF2 protein levels in postnatal (P) and adult (Ad) mouse quadriceps at the indicated time of development. γ-tubulin and Ponceau S-stained blots are shown as loading controls. (b) Cells exposed to GM and DM for indicated times were immunostained for GRAF2. Note increased expression during C2C12 differentiation and recruitment of GRAF2 to pre-fusion complexes (*arrows*). Scale bars=50 μm. Bottom panels are high magnification images that reveal co-localization of GRAF2 and myoferlin at the tip of a myoblast exposed to DM for 48 h. (c) $GRAF1^{+/+}$ and $GRAF1^{gt/gt}$ primary myoblasts transfected with GRAF2-specific or control (NTC) siRNA and exposed to DM for 36 h were assessed for GRAF2 and GRAF1 expression by reverse transcriptase-PCR. GAPDH is shown as a loading control. (d) $GRAF1^{+/+}$ primary myoblasts depleted of GRAF2 by siRNA knockdown exhibited reduced nuclear accretion in comparison to NTC-treated control $GRAF1^{+/+}$ myoblasts. Moreover, depletion of GRAF2 in $GRAF1^{gt/gt}$ cells exhibited a further reduction in nuclear accretion in

comparison to NTC-treated GRAF1$^{+/+}$ and GRAF1$^{gt/gt}$ myoblasts ($^{*}p < 1 \times 10^{-4}$, $^{**}p < 0.005$, $^{\#}p < 0.05$, n.s. = not significant; n=300 cells per condition, N=3 independent experiments). (e) C2C12 cells were transfected with control (NTC), GRAF1-, GRAF2-, or both GRAF1- and GRAF2-specific siRNAs and exposed to DM for 36 h before being lysed and immunoblotted with a GRAF2 antibody to assess protein knockdown efficiency. γ-tubulin is shown as a loading control. (f) Quantification of the EHD1 fluorescence ratio (refer to Fig. 7f and methods for details) in C2C12 cells transfected with control (NTC), GRAF1-, GRAF2-, or both GRAF1- and GRAF2-specific siRNAs that were exposed to DM for 36 h and immunostained for EHD1 and Tm to demarcate differentiated myoblasts ($^{*}p < 0.05$, $^{**}p < 0.005$; n=50 cells per condition, N=3 independent experiments). Data are mean ± s.e.m. Scale bars =10 μm, unless otherwise indicated.